STIFFENED SPRINGBACK REFLECTORS

L.T. Tan and S. Pellegrino

Department of Engineering, University of Cambridge
Trumpington Street, Cambridge, CB2 1PZ, U.K.
pellegrino@eng.cam.ac.uk

ABSTRACT: The recently developed Spring Back Reflector has low stiffness in the deployed configuration. A general method of stiffening this type of reflector without changing its folding properties is presented. The stiffening is achieved by adding a conical skirt around the edge of the dish; this skirt snaps elastically when the dish is folded. The paper concludes that it is possible to design spring back reflectors that are up to 80 times stiffer and with a deployed fundamental frequency up to 8 times higher than in the original design.

INTRODUCTION

The newly developed Spring Back Reflector [1], shown schematically in Fig. 1, consists of a thin-walled graphite mesh dish with an integral lattice of ribs and connecting elements. These components, together with a further stiffening edge beam along the rim, are made from triaxial plies of carbon-fibre reinforced plastic (CFRP). The whole structure is made as a single piece, without any expensive and potentially unreliable joints, and typically has a diameter of 6 m, thickness varying between 0.3 mm and 3.2 mm, and a total mass of around 20 kg.

The folding concept is both simple and effective: since there are no joints or hinges, opposite edges of the reflector are pulled towards each other by about half of their original distance, and thus the reflector becomes folded elastically as shown in Fig. 1. It can then be stowed in the normally unused space in the nose cone of a rocket launcher. Once in orbit, the tie cables that hold the reflector in its packaged configuration are released, and the reflector deploys dynamically by releasing its stored elastic strain energy.
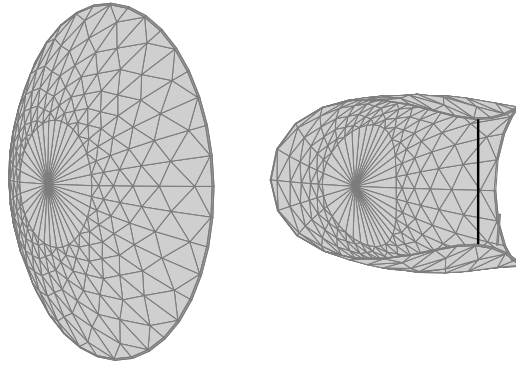

Figure 1: Schematic views of spring-back reflector, folded and deployed.

In order to be folded as described, Spring Back Reflectors need to have low stiffness but it is precisely their low stiffness that makes it difficult for them to achieve and retain a high shape accuracy. Furthermore, shape distortions that occur during the manufacturing of thin CFRP structures —of the order $D/1000$ in the present case— make it even more difficult to meet the stringent shape accuracy requirements imposed on communications antennas. This is a significant problem, and potentially a severe limitation on the applicability of this type of reflector. The surface accuracy of the reflector could be adjusted with mechanical devices, but this would defy the simplicity of the concept and reduce the reliability of the system.

This paper proposes a modification of the original concept, based on the idea of adding a thin-walled stiffening element around the edge of the dish. This element significantly increases the overall stiffness of the dish in the deployed configuration, and yet its configuration is such that the stiffened dish can still be folded elastically. A detailed finite element study is presented of the effects of changing the various parameters of the stiffening element from which optimal configurations of a $1/10^{\text{th}}$ scale model —i.e. about 0.5 m diameter— reflector are
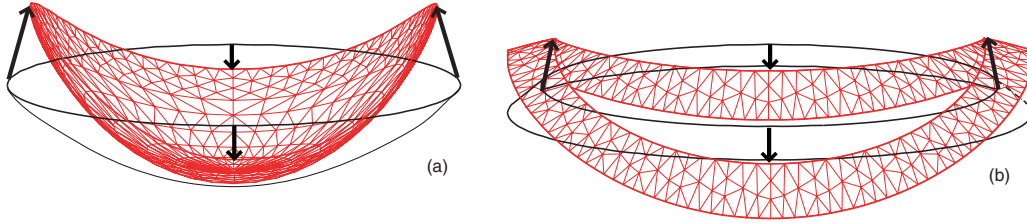
Figure 2: Lowest stiffness, incompatible eigenmodes of dish and skirt.

chosen. Two selected configurations have been physically realized and their measured properties are compared with finite element predictions.

STIFFENING METHOD

In general, the stiffer one makes a linear-elastic structure, the "harder" it becomes to fold it elastically. This intuitive statement can be formalized using an argument based on the total strain energy in the structure being equal to the work done by two equal and opposite forces that are applied to the structure in order to fold it. If the "stiffness" is increased, the strain energy required to fold the structure by a given amount will increase proportionally. The maximum stress in the structure will also increase.

A spring-back reflector could be stiffened by increasing the stiffness of the edge rim or the ribs. However, increasing the thickness of these elements has the effect of rapidly increasing the maximum stress level in the folded reflector, whereas increasing their width is inefficient in terms of mass.

An alternative, more efficient way of increasing the stiffness of a structure is to prevent it from deforming in its lowest stiffness eigenmode. In the case of an "open cap" shell this eigenmode is the inextensional, or first bending mode sketched in Fig. 2(a). The associated eigenfrequency can be substantially increased by connecting the original shell to a second shell whose lowest stiffness eigenmode is geometrically incompatible with that of the first shell. In Fig. 2(b) a conical shape has been chosen.

In practice, this amounts to adding a conical skirt around the original reflector, but the addition of a continuous skirt would make the reflector so stiff that it would no longer be possible to fold it. Therefore, following an approach put forward in [2] , we counteract this effect by introducing a series of cuts, either in the skirt or in the connection between the skirt and the dish.

DESIGN OPTIMIZATION

In order to work out a proper solution based on the approach proposed above, we need to carry out a more formal search of the design space. Fig. 3 defines the five parameters to be optimised, which are

- the angles α, β defining the length of the two sets of slits;
- the angle γ defining the inclination of the skirt;
- the width w of the skirt; and
- the length of the cuts (which can be either 0 or w).

All of these parameters, apart from the length of the cuts, can be varied over a wide range; more details are given later in this section.

Due to the number of parameters to be optimized and the complexity of each step in the optimization process, considering a simultaneous variation of all parameters is not feasible. Hence, two types of designs, which had shown the most promise during the preliminary study, were selected and for each design optimal configurations were sought. These two designs are as follows.

- Configuration A. Two cuts and four slits of equal length ($\alpha = \beta$).
- Configuration B. Four slits of general lengths ($\alpha \neq \beta$), but no cuts.
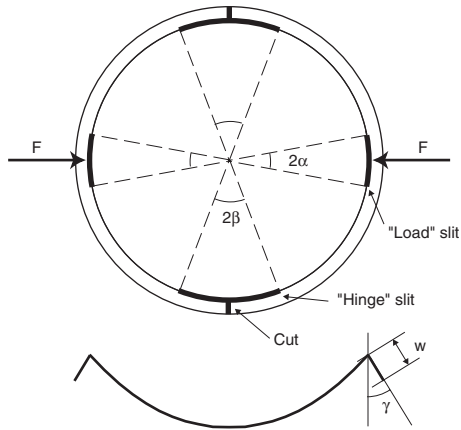
Optimization Routine
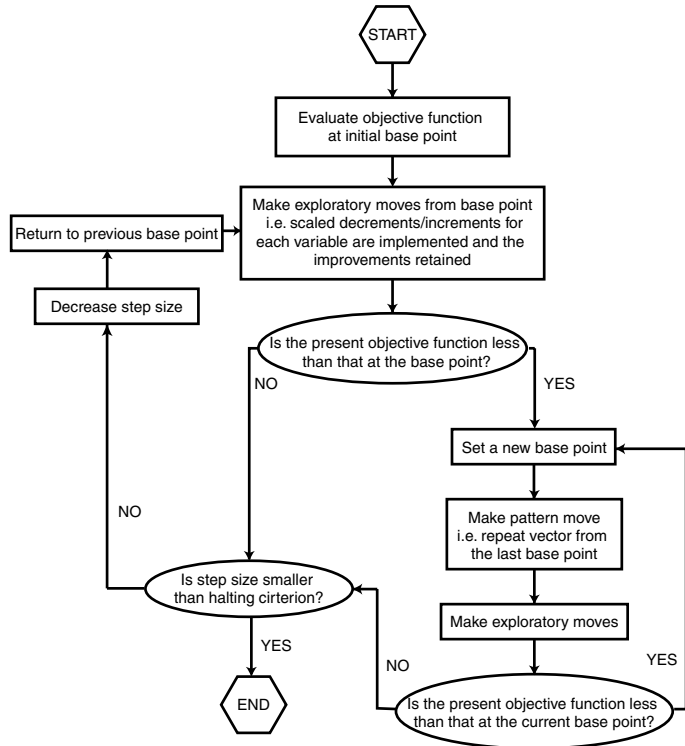
Figure 3: Design parameters.

Figure 4: Flow chart of Hooke and Jeeves method.

Because there is no known analytical relationship between the design parameters, the easiest approach is the direct search method. The particular optimization method that was chosen was the Hooke and Jeeves (HJ) method [3], which has the advantage of not requiring the evaluation of gradients of the objective function and hence is particularly suited for problems where solutions can only be obtained numerically.

Fig. 4 lists the various steps and decisions involved in this search method. It is available as a routine, written in C [4].

Automatic Generation of Stiffening System

To carry out the optimization, an automatic method of changing the design parameters which does not require any user input was needed. For each of the two basic designs defined previously there are four parameters to be optimized, namely $\alpha, \beta, \gamma,$ and w. It is worth noting that none of these parameters affects the shape and design of the actual dish of the reflector; it is intended that the addition of the skirt be a relatively minor modification of the spring back reflector design. With this in mind, a quarter mesh of general 3 node shell elements (S3R) was generated for the reflector dish with PATRAN [5] and then written to an ABAQUS [6] input file. The nodes of this mesh were uniformly spaced on the rim, at an angle of 2 deg apart; the total number of nodes was around 600.

The skirt was then generated directly in the model input file by defining a generator starting at a point P on the rim of the dish and ending at point Q, see Fig. 5. Varying the position of Q enables us to vary both the skirt angle, γ, and the skirt width, w. This generator is then rotated around the axis of the dish to define the skirt nodes in such a way that the nodes on the inner edge of the skirt are colocated with those on the rim of the dish. If cuts are to be introduced in the skirt, each separate portion is formed separately. The skirt and the dish are then connected by using the type "TIE" from the "MULTI POINT CONSTRAINT" option in ABAQUS. This option equates the global displacements and rotations of the two nodes that are tied together.

A simple way of modelling a slit would be to leave the corresponding nodes untied. However this would allow us to consider only slit lengths that are an exact multiple of the distance between rim nodes. Instead,
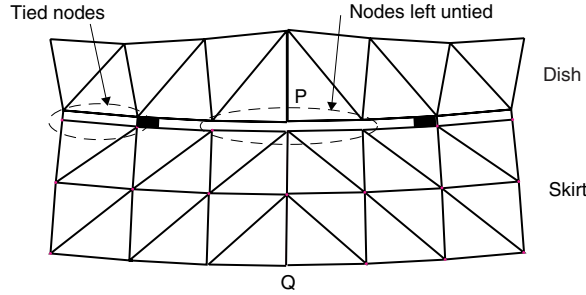
3

Figure 5: Schematic of automatic mesh generation.

two additional, smaller shell elements were generated, one between each end of the slit and the first pair of dish/skirt nodes. The location of these smaller elements is calculated by a routine which, for a given set of design parameters, locates the two sets of standard dish/skirt nodes between which the end of the slit occurs. This allows the length of the slit to be varied continuously. Finally, the nodes at the end of the slit are connected to the rest of the model by using the "LINEAR" option from the ABAQUS "MULTI POINT CONSTRAINT" function. This option specifies the rotation and the displacement of a given node as a proportion of the two nodes on either side of it.

This method of automatically generating the slits was tested by considering a configuration in which the slits terminated exactly at a dish/skirt node. Hence, for this case it was possible to use the simpler modelling technique described previously. The frequencies obtained from the two methods differed by 0.18%. The difference being due to the fact that the slit in the automatic meshing method leaves a small void in the skirt and hence the mass of this configuration is slightly lower.

ABAQUS Simulation

After setting up the ABAQUS input file two different analyses were carried out. First, the fundamental natural frequency of the structure was determined from a linear eigenvalue analysis, and second a geometrically non-linear, displacement controlled simulation of the folding process was performed, in order to find the maximum stress in the structure.

Given a structure that exhibits snapping behaviour, in general it is not obvious at which stage of folding the maximum stress, σ_{max}, will be reached. In the present case, though, an exhaustive numerical study had shown that —due to the very large deformation that is imposed after any snaps have taken place— σ_{max} for the dish occurs always in the final, fully-folded configuration of the reflector. Typically, in this configuration the two diametrically opposite points of the reflector that are pushed closer together are at a distance of $D/2$. Therefore, only the stresses in the final configuration need to be scanned by the interface routine to find σ_{max}, at the end of the folding simulation.

Objective Function

The aim of the optimization is to maximise the fundamental natural frequency of vibration of the deployed structure, subject to a limit, σ_0, on the maximum stress in the structure in the folded configuration. This limit was implemented through a penalty function which greatly increases the objective function if the limit is exceeded. Mathematically, this can be expressed as:

$$F_{obj} = -f + \exp(\sigma_{max} - \sigma_0) \tag{1}$$

OPTIMIZATION RESULTS

A 1 mm thick, parabolic dish with the following properties was optimized: diameter $D = 450$ mm, focal length $F = 135$ mm, made from Polyethylene Terephthalate Glycol Modified, PETG (sold in sheet form, under the trade name Vivak). This material is essentially isotropic and has Young's Modulus $E = 1.86$ GPa and Poisson's ratio $\nu = 0.36$.

4

The following limits were placed on the design parameters of the stiffening system

- slit angles, $0.5 \leq \alpha, \beta \leq 30$ deg;
- skirt angle, $-5 \leq \gamma \leq 150$ deg;
- skirt width, $5 \leq w \leq 40$ mm.

and both Configuration A and Configuration B were investigated for different values of σ_0.

Optimal values were found to have at least a factor of 3 increase in fundamental natural frequency, compared to the unstiffened configuration (which has $f_0 = 5.8$ Hz) for $\sigma_0 = 25$ MPa, increasing to nearly 8 for $\sigma_0 = 40$ MPa. This optimization problem does not have a single minimum, hence to be reasonably sure that convergence to the global optimum has been achieved, for a particular value of σ_0 several optimization runs —typically 10 or more— were carried out with different starting points. At the end, the solutions with the highest frequency were selected. It was noted that the optimization usually converges to the maximum value of w, and hence in some optimization runs w was assigned a definite value, instead of being considered as a variable.

Fig. 6 is a plot of the eight optimal values obtained, initially by prescribing different values for σ_0 only —points 1 to 4— and then by also prescribing $w = 20$ mm —points 5 to 8. The corresponding design parameters are listed in Table 1. Note that all eight designs have $\gamma \approx 90$ deg and there is a general trend for γ to decrease with increasing σ_0.

Consider the optimal configuration with $\sigma_0 = 40$ MPa, i.e. point 3 in Fig. 6; this configuration has $w = 40$ mm. Dividing w by 2 results in a 40% decrease in f, see point 8. Points 5-8 in Fig. 6 show clearly that the rate of increase in f in the optimal configurations is much lower than the associated increase in σ_0; the slope of a best-fit line through points 5-8 is $\approx 1 : 5$. The gentle slope of this line, compared to the sharp curve between points 1-3, is due to the fact that the configurations with $w = 20$ mm are able to reach the maximum attainable stiffness for the given stress limit, whereas the configurations with $w = 40$ mm are governed by the stress limit.

In conclusion, the general trend is

- if σ_0 is the controlling factor, $\gamma \geq 90$ deg;
- if σ_0 is easily achievable, $\gamma \leq 90$ deg.

This is because pointing the skirt below the level of the rim of the unstiffened dish is a more efficient way of increasing the stiffness against first-mode deformation, but also produces higher stress levels during folding.

The highest stresses in a folded reflector tend to concentrate around the edge of the slit; about 90% of the structure is typically at a stress that is 40% lower. It should be noted that —in calculating the highest stress— the elements at the tips of the slits have been ignored as there is a stress concentration that could be removed simply by rounding the sharp end of the slits. Since PETG has an ultimate failure stress of around 50 MPa, it was decided to choose $\sigma_0 = 25$ MPa. At this point, the final choice of w involved a trade-off between added mass and stiffness increase. Table 2 compares three different configurations, all with a stress limit of 25 MPa.

A similar optimization study was carried out for Configuration A, with two cuts across the skirt and four slits subtending equal angles. This configuration tends to suffer from higher stress concentrations, and so it is more difficult to find design parameters for which the yield stress of the material is not exceeded. To alleviate this problem, the six most highly stressed nodes in the finite element model, which correspond to a small area

Table 1: Optimal configurations

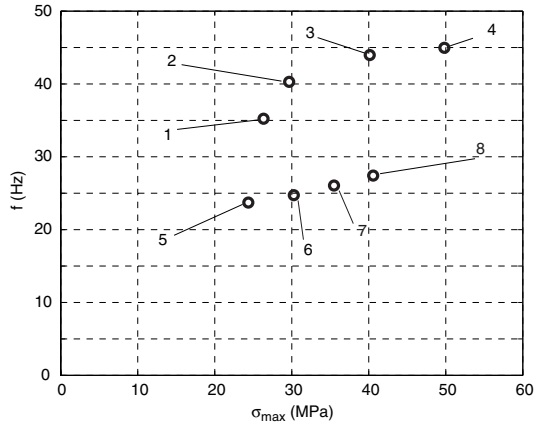| Point	α (deg)	β (deg)	γ (deg)	w (mm)	f (Hz)	σ_{max} (MPa)
1	0.1	14.9	93.7	39.5	35.2	26.2
2	2.3	13.2	90.3	40.0	40.2	30.0
3	0.5	9.1	88.9	40.0	43.8	40.1
4	0.5	6.8	88.6	39.8	45.0	49.7
5	6.1	17.4	88.1	20.0	24.0	25.3
6	4.0	14.8	87.9	20.0	24.8	30.5
7	4.1	11.4	87.5	20.0	26.2	35.4
8	2.8	10.6	86.7	20.0	27.0	40.5

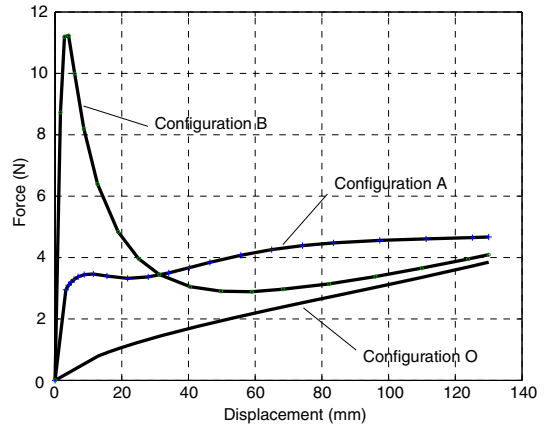Figure 6: Trade off between f and σ_{max} for Configuration B.

Figure 7: Comparison of three configurations.

around the tip of the cut, were disregarded in the calculation of σ_{max}, again on the grounds that high stress concentration issues could be dealt with by a more careful design of the details. The outcome is that all optimal designs for this configuration have $\gamma > 90$ deg.

Fig. 7 compares the force-displacements relationships of two optimized configurations, A and B, with that of the original configuration, O. Note that the displacement plotted on the abscissa is for only one edge of the dish, hence the distance between the edges that are brought together during folding changes by twice this amount. Both of the optimized configurations have $\sigma_{max} = 49.6$ MPa and $w = 40$ mm. Configuration A has $\alpha = \beta = 0.5$ deg, $\gamma = 95$ deg, and $f = 17.6$ Hz. Configuration B has $\alpha = 0.5$ deg, $\beta = 6.8$ deg, $\gamma = 89$ deg, and $f = 45$ Hz..

Note that both configuration A and B are much stiffer than O near the origin, but then snap and for larger displacements tend towards the force-displacement curve of Configuration O. The force required to hold these reflectors fully folded is only a little higher than for the original reflector, by 12% for Configuration A and 7% for Configuration B. It should be noted that the snapping behaviour that is exhibited by these optimized designs is generally not seen in non-optimized structures.

In conclusion, Configuration B has the most promise and makes it comparatively easy to achieve a high stiffness with stresses below any given limit. This is because this configuration allows longer slits in the regions of highest elastic curvature of the reflector, which has the effect of distributing the strain over a wider region thus decreasing the peak strain. On the other hand, the presence of a radial cut in the skirt, in Configuration A, tends to form a hinge-like region along the axis of bending, which is responsible for higher, localised strains.

EXPERIMENTAL VERIFICATION

In order to verify selected results from the optimization study, two types of experiments were carried out on small scale physical models:

- static compression tests, to characterize both the initial stiffness of the structure and the force-displacement

Table 2: Mass and frequency for $\sigma_{max} = 25$ MPa

w (mm)	Additional Mass (% of original)	f/f_0 (Hz)
20	16	4.1
30	24	5.3
40	33	5.9

Table 3: Tested configurations

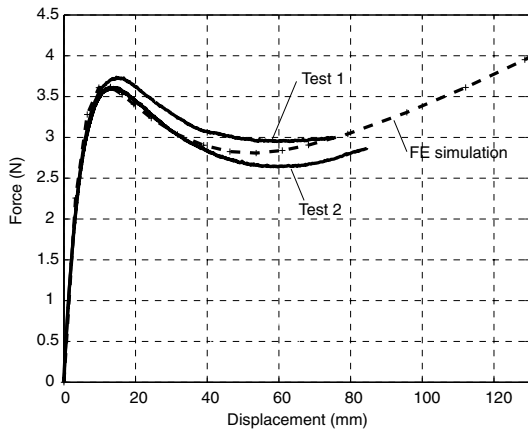| Configuration	Cuts	Slits	α (deg)	β (deg)	γ (deg)	w (mm)
O	-	-	-	-	-	-
A	2	2	-	4	50	20
B	-	4	8	24	90	20

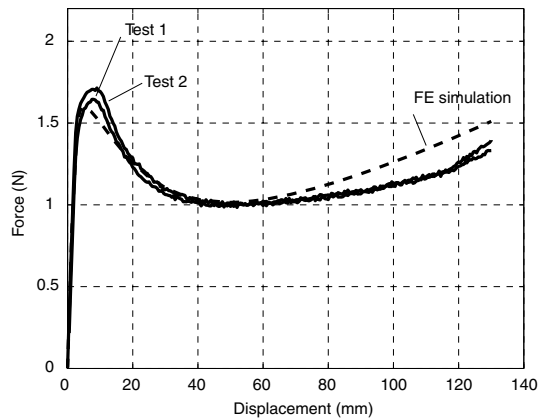Figure 8: Comparison of two tests on Configuration A dish with FE analysis.

Figure 9: Comparison of two tests on Configuration B dish with FE analysis.

relationship during folding;

• vibration tests, to measure the natural frequencies of the structure.

These experiments were carried out on PETG dishes made by vacuum forming on parabolic moulds with conical edges. The exact dimensions of these moulds were, diameter $D = 452$ mm, focal length $F = 134$ mm and skirts angles of 50 or 90 deg. Further details are given in Table 3.

Figs 8 and 9 show the force-displacement plots of the two stiffened configurations that were tested —see Table 3 for details on the corresponding design parameters— and compares them to the ABAQUS simulations. Note that both tests of the Configuration A dish were stopped before attaining the completely packaged shape, to prevent permanent damage of the dish.

In both cases there is excellent correlation between experimental and computational results. The initial slope of the graphs, corresponding to the stiffness of the dishes, has been simulated very accurately. Note that there is a 4% experimental scatter in the peak force of the Configuration A dish, Fig. 8, which tends to increase in the post-buckling range. In Fig. 9 the scatter is smaller, and it can be noted that the experimental model buckles marginally later and at a slightly larger load. Considering that we are dealing with the large-displacement behaviour of thin shell structures, which are notoriously challenging to model, these discrepancies are too small to worry about.

Table 4 lists the measured frequencies of the first bending mode of the three configurations listed in Table 3. For Configuration B the measurements were taken with the dish suspended horizontally "cup up". These values are compared first with ABAQUS predictions in vacuum and in air. The last column gives the error between the measurements and the predicted frequencies in air.

The results presented in this section have provided an experimental validation for the finite element simulation technique used for the optimization study. Thus, having confirmed that both the large displacement load-displacement relationship and the first bending frequency of a stiffened reflector were computed very accurately by the simulation, it can now be expected that the predictions will be equally accurate for other designs of stiffened reflectors.

Table 4: Frequency results (Hz)

Configuration	Exp.	ABAQUS (vacuum)	ABAQUS (air)	Error (%)
O	5.0	5.8	4.8	4.4
A	14.9	17.0	15.0	1.1
B	15.4	16.8	14.9	3.3

Of the two stiffened reflectors that have been tested, neither of which had particularly well optimized design parameters, Configuration B has been confirmed to be the most promising. Although the two configurations have achieved essentially identical stiffness and natural frequency in the deployed configuration, the Configuration A dish gave some concern during folding, and so the fully-folded configuration was never reached for this one. On the other hand, the Configuration B dish was folded many times without difficulty.

CONCLUSIONS

The stiffness in the deployed configuration of a Spring Back Reflector can be increased significantly without compromising its ability to fold elastically.

A particular stiffening system has been proposed and evaluated. In its most successful implementation, it consists of a thin-walled conical shell structure that is attached to the edge of the reflector dish. By introducing short discontinuities between the dish and the stiffening element, the behaviour of the stiffening system can be tuned in order to maximize the increase in stiffness in the deployed configuration while minimizing the increase in the maximum stress in the fully-folded configuration. Determining the optimal parameters, i.e. the width and angle of the stiffening structure as well as the length of the discontinuities along the attachment to the dish, requires extensive non-linear finite element simulations and a careful optimization. However, as a first approximation a flat stiffening structure perpendicular to the axis of the reflector is likely to be near-optimal.

Ten-fold increases in stiffness and three-fold increases in the first bending frequency of a small-scale reflector have been verified experimentally. Optimized designs with 80-fold stiffness increases and 8-fold frequency increases have been shown to be possible. Preliminary results for full-scale reflectors, not shown in this paper, suggest that similar improvements can be achieved at full scale.

ACKNOWLEDGEMENTS

REFERENCES

[1] Anonymous, "Hughes graphite antennas installed on MSAT-2 craft," *Space News*, November 1994.

[2] Greschik, G., "On the practicality of a family of pop-up reflectors," *9th Annual AIAA/Utah State University Conference on Small Satellites*, 18-21 September 1995.

[3] Hooke, R. and Jeeves, T.A., "Direct search solution of numerical and statistical problems," *Journal of ACM*, Vol. 8, April 1961, pp. 212–229.

[4] Johnson, M.G., "hooke.c," http://netlib.bell-labs.com/magic/netlib_find?db=0&pat=hooke+jeeves+.

[5] *MSC/PATRAN Version 8.5*, MacNeal-Schwendler Corporation, Los Angeles, California, USA, 1999.

[6] *ABAQUS Version 6.1*, Hibbitt, Karlsson & Sorenson, 1080 Main Street, Pawtucket, RI 02860-4847, USA, 1998.